COMPUTATIONAL METHODS IN ENGINEERING
2nd Asia-Pacific Int. Conf. on Comp. Meth. in Engrg (ICOME 2006)
Nov. 14-16, 2006, Hefei, China

Some Recent Results of the Null-Field Integral Equation Approach for Engineering Problems with Circular Boundaries

Jeng-Tzong Chen *

Department of Harbor and River Engineering, National Taiwan Ocean University, Keelung 20224, Taiwan, China

E-mail: jtchen@mail.ntou.edu.tw

Abstract In this paper, a systematic approach is proposed to deal with engineering problems containing circular boundaries. The mathematical tools, degenerate kernels and Fourier series, are utilized in the null-field integral formulation. The kernel function is expanded to the degenerate form and the boundary density is expressed into Fourier series. By collocating the null-field point on the real boundary, the singularity is novelly avoided. Five gains of well-posed model, singularity free, boundary-layer effect free, exponential convergence and mesh-free approach are achieved. By matching the boundary condition, a linear algebraic system is obtained. After obtaining the unknown Fourier coefficients, the solution can be obtained by using the integral representation. This systematic approach can be applied to solve the Laplace, Helmholtz, bi-Helmholtz and biharmonic problems. Besides, the circular inclusions as well as the electro-elastic coupling of piezoelectricity are addressed. Finally, several examples, including Stokes' flow, elasticity and piezoelectricity, are demonstrated to show the validity of present formulation.

INTRODUCTION

Engineering analysis can be formulated as mathematical models of the boundary value problems. In order to solve the boundary value problems, researchers and engineers have paid more attention on the development of boundary integral equation method (BIEM), boundary element method (BEM) and meshless method than domain type methods, finite element method (FEM) and finite difference method (FDM). Among various numerical methods, BEM is one of the most popular numerical approaches for solving boundary value problems. Although BEM has been involved as an alternative numerical method for solving engineering problems, five critical issues are of concern.

(1) *Treatment of singularity and hypersingularity* It is well known that BEM are based on the use of fundamental solutions to solve partial differential equations. These solutions are two-point functions which are singular as the source and field points coincide. Most of the efforts have been focused on the singular boundary integral equation for problems with ordinary boundaries. In the past, several regularizations for hypersingularity were offered to handle it in direct and indirect ways. In the present approach, we employed the degenerate kernel to represent the two-point fundamental solution for problems with circular boundaries. The singularity and hypersingularity disappeared in boundary integral equation after describing the potential into two parts. The idea of changing real boundary to fictitious boundary (fictitious BEM) or putting the observation point outside the domain (null-field approach) can remove the singular and hypersingular integrals. However, they result in an ill-posed matrix which will be elaborated on later.

(2) *Boundary-layer effect* Boundary-layer effect in BEM has received attention in the recent years. In real applications, data near boundary can be smoothened since maximum principle always exists for potential problems. Nevertheless, it also deserves study to know how to manipulate the nearly singular integrals in applied mathematics. Many regularization techniques can be found in the literature. How to eliminate the boundary-layer effect in BEM is vital for researchers.

(3) *Convergence rate* Undoubtedly, BEM is very popular for boundary value problems with general geometries since it requires discretization on the boundary only. Regarding to constant, linear and quadratic elements, the

discretization scheme does not take the special geometry into consideration. It leads to the slow convergence rate. For example, Fourier series is suitable for boundary densities on circular boundaries while the spherical harmonic function is always employed to approximate the boundary density on surface of sphere. Although previous researchers have employed the Fourier series expansion, no one has ever introduced the degenerate kernel in boundary integral equations to tackle their problems. Mathematicians have proved that the exponential convergence instead of the algebraic convergence in the BEM can be achieved by using the degenerate kernel and Fourier expansion.

(4) *Ill-posed model* As mentioned previously in the first issue, to avoid directly calculating the singular and hypersingular integrals by using null-field approach or fictitious BEM yields an ill-condition system. The influence matrix is not diagonally dominated and needs preconditioning. To approach the fictitious boundary to the real boundary or to move the null-field point to the real boundary can make the system well-posed. However, singularity appears in the meantime. We may wonder is it possible to push the null-field point on the real boundary but free of facing the singular or hypersingular integrals. The answer is yes and can be found in this paper.

(5) *Mesh on boundary is still necessary*.

To develop a BEM with several advantages, singularity free, the suppression of boundary-layer effect, exponential convergence, well-posed model and mesh-free is the main motivation of this paper.

Engineering problems with circular boundaries are often encountered, *e.g.* missiles, aircraft, naval architecture, etc., either to reduce the weight of the whole structure or to increase the range of inspection as well as piping purposes. Analytical approach using bi-polar coordinate [1] was developed for two-hole problems. Complex variable techniques were also employed for the annular case. For a problem with several holes, many numerical methods, *e.g.* finite element method (FEM) and boundary element method (BEM), were resorted to solve. To develop a systematic approach for engineering problems with circular boundaries is not trivial.

Null-field integral equation approach is used widely for obtaining the numerical solutions to engineering problems. Various names, *e.g.* T-matrix method [2] and extended boundary condition method (EBCM) [3], have been coined. A crucial advantage of this method consists in the fact that the influence matrix can be computed easily. Although many works for acoustic and water wave problems have been done, we focus on the solid mechanics here.

In this paper, we review the recent development of the null-field integral equation approach [4-10] for boundary value problems (BVPs) with circular boundaries. The key idea is the expansion of kernel functions and boundary densities in the null-field integral equations. Vector decomposition technique using the adaptive observer system is required for nonlocal cases. Applications to the Laplace, Helmholtz, biharmonic and bi-Helmholtz problems are addressed. Not only interior problems but also exterior cases are solved. Emphases on the inclusion problems as well as piezoelectricity studies are done. Several examples were demonstrated to see the validity of the new formulation.

NULL-FIELD INTEGRAL EQUATION APPROACH FOR BOUNDARY VALUE PROBLEMS

Suppose there are N randomly distributed circular boundaries bounded to the domain D and enclosed with the boundary, B_k ($k = 0, 1, 2, \cdots, N$) as shown in Fig. 1. We define

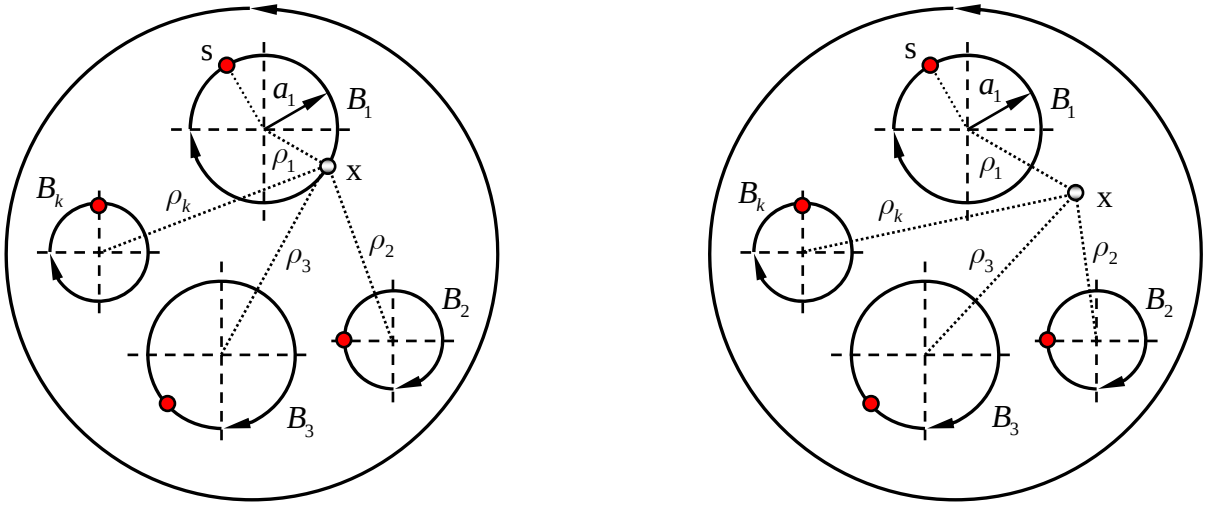

Figure 1: Sketch of null-field and domain points in conjunction with the adaptive observer system (left: collocation on the boundary point, right: collocation on the interior point)

$$B = \bigcup_{k=0}^{N} B_k \ . \tag{1}$$

In mathematical physics, boundary value problems can be modelled by the governing equation,

$$\mathcal{L}\, u(\mathrm{x}) = 0\,, \quad \mathrm{x} \in D\,, \tag{2}$$

where $\mathcal{L}$ may be the Laplace, Helmholtz, biharmonic or bi-Helmholtz operator, $u(\mathrm{x})$ is the potential function and D is the domain of interest. For the 2-D Laplace and Helmholtz problem, the integral equation for the domain point can be derived from the third Green's identity, we have

$$2\pi u(\mathrm{x}) = \int_B T(\mathrm{s},\mathrm{x}) u(\mathrm{s}) dB(\mathrm{s}) - \int_B U(\mathrm{s},\mathrm{x}) t(\mathrm{s}) dB(\mathrm{s}),\ \mathrm{x} \in D, \tag{3}$$

$$2\pi \frac{\partial u(\mathrm{x})}{\partial \mathrm{n}_{\mathrm{x}}} = \int_B M(\mathrm{s},\mathrm{x}) u(\mathrm{s}) dB(\mathrm{s}) - \int_B L(\mathrm{s},\mathrm{x}) t(\mathrm{s}) dB(\mathrm{s}),\ \mathrm{x} \in D, \tag{4}$$

where s and x are the source and field points, respectively, $t = \partial u / \partial \mathrm{n}$, B is the boundary, n_{x} denotes the outward normal vector at the field point x and the kernel function $U(\mathrm{s},\mathrm{x})$, is the fundamental solution, and the other kernel functions, $T(\mathrm{s},\mathrm{x})$, $L(\mathrm{s},\mathrm{x})$ and $M(\mathrm{s},\mathrm{x})$, are defined in the dual boundary integral method (BIEM) [10]. It is noted that more potentials are needed in Eqs. (3) and (4) for biharmonic and bi-Helmholtz cases [6, 19].

By moving the field point to the boundary, the Eqs. (3) and (4) reduce to

$$\pi u(\mathrm{x}) = C.P.V. \int_B T(\mathrm{s},\mathrm{x}) u(\mathrm{s}) dB(\mathrm{s}) - R.P.V. \int_B U(\mathrm{s},\mathrm{x}) t(\mathrm{s}) dB(\mathrm{s}),\ \mathrm{x} \in B, \tag{5}$$

$$\pi \frac{\partial u(\mathrm{x})}{\partial \mathrm{n}_{\mathrm{x}}} = H.P.V. \int_B M(\mathrm{s},\mathrm{x}) u(\mathrm{s}) dB(\mathrm{s}) - C.P.V. \int_B L(\mathrm{s},\mathrm{x}) t(\mathrm{s}) dB(\mathrm{s}),\ \mathrm{x} \in B, \tag{6}$$

where *C.P.V.*, *R.P.V.* and *H.P.V.* denote the Cauchy principal value, Riemann principal value and Hadamard principal value, respectively. By collocating the field point x outside the domain (including boundary), the null-field integral equations yield

$$0 = \int_B T(\mathrm{s},\mathrm{x}) u(\mathrm{s}) dB(\mathrm{s}) - \int_B U(\mathrm{s},\mathrm{x}) t(\mathrm{s}) dB(\mathrm{s}),\ \mathrm{x} \in D^c \cup B, \tag{7}$$

$$0 = \int_B M(\mathrm{s},\mathrm{x}) u(\mathrm{s}) dB(\mathrm{s}) - \int_B L(\mathrm{s},\mathrm{x}) t(\mathrm{s}) dB(\mathrm{s}),\ \mathrm{x} \in D^c \cup B, \tag{8}$$

by choosing appropriate forms of degenerate kernels, where D^c is the complementary domain.

EXPANSIONS OF THE FUNDAMENTAL SOLUTION AND BOUNDARY DENSITY

Instead of directly calculating the *C.P.V.*, *R.P.V.* and *H.P.V.* in Eqs.(5) and (6), we obtain the linear algebraic system from the null-field integral equations of Eqs.(7) and (8) through the kernel expansion.

Based on the separable property, the kernel function $U(\mathrm{s},\mathrm{x})$ can be expanded into the separable form by dividing the source and field point:

$$U(\mathrm{s},\mathrm{x}) = \begin{cases} U^i(\mathrm{s},\mathrm{x}) = \sum_{j=1}^{\infty} A_j(s) B_j(x), & |\mathrm{s}| \geq |\mathrm{x}|, \\ U^e(\mathrm{s},\mathrm{x}) = \sum_{j=1}^{\infty} A_j(x) B_j(s), & |\mathrm{x}| > |\mathrm{s}|, \end{cases} \tag{9}$$

where the $A(\mathrm{x})$ and $B(\mathrm{x})$ can be found for the Laplace [4, 7-9], Helmholtz [5], biharmonic [6] and bi-Helmholtz [19] operators and the superscripts "i" and "e" denote the interior ($|\mathrm{s}| \geq |\mathrm{x}|$) and exterior ($|\mathrm{x}| > |\mathrm{s}|$) cases, respectively. To classify the interior and exterior regions, Fig. 2 shows for one, two and three dimensional cases. For the degenerate form of T, L and M kernels, they can be derived according to their definitions.

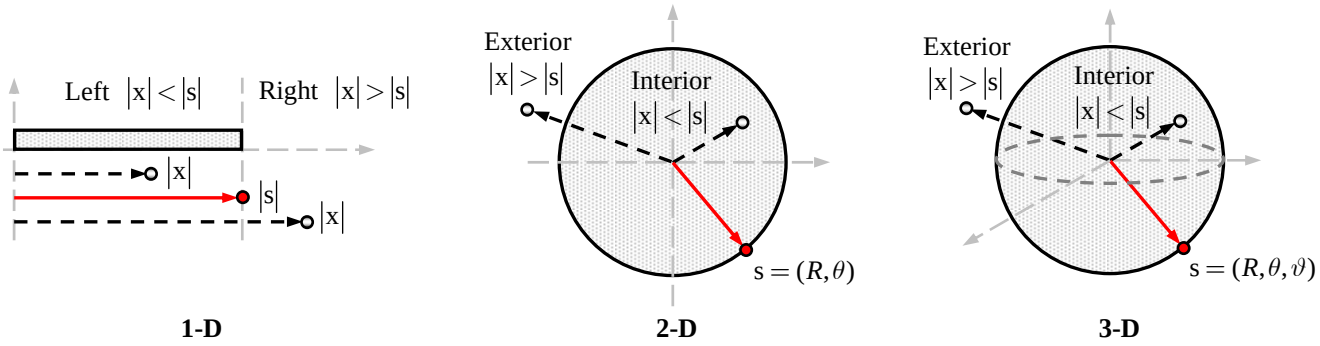

Figure 2: The degenerate kernel for the one, two and three dimensional problems

We apply the Fourier series expansions to approximate the potential u and its normal derivative t on the B_k circular boundary

$$u(\mathrm{s}_k) = a_0^k + \sum_{n=1}^{m} (a_n^k \cos n\theta_k + b_n^k \sin n\theta_k), \mathrm{s}_k \in B_k, k = 0, 1, 2, \cdots, N, \tag{10}$$

$$t(\mathrm{s}_k) = p_0^k + \sum_{n=1}^{m} (p_n^k \cos n\theta_k + q_n^k \sin n\theta_k), \mathrm{s}_k \in B_k, k = 0, 1, 2, \cdots, N, \tag{11}$$

where a_n^k, b_n^k, p_n^k and q_n^k $(n = 0, 1, 2, \cdots)$ are the Fourier coefficients and θ_k is the polar angle measured with respect to the x-direction.

After collocating the null-field points in the null-field integral equation of Eq. (7), the boundary integrals through all the circular contours are required. It is worth noting that the origin of the observer system is located on the center of the corresponding circle under integration to entirely utilize the geometry of circular boundary for the expansion of degenerate kernels and boundary densities. Figure 1 shows the boundary integration for the circular boundaries in the adaptive observer system.

By collocating the null-field point x_k on the kth circular boundary for Eq. (7) in Fig. 1, we have

$$0 = \sum_{k=0}^{N} \int_{B_k} T(\mathrm{s}_k, \mathrm{x}_j) u_k(\mathrm{s}) dB_k(\mathrm{s}) - \sum_{k=0}^{N} \int_{B_k} U(\mathrm{s}_k, \mathrm{x}_j) t_k(\mathrm{s}) dB_k(\mathrm{s}), \mathrm{x} \in D^c, \tag{12}$$

where N is the number of circular boundaries including the outer boundary and the inner boundaries. Therefore, a linear algebraic system is obtained

$$[\mathbf{U}]\{\mathbf{t}\} = [\mathbf{T}]\{\mathbf{u}\}, \tag{13}$$

where $[\mathbf{U}]$ and $[\mathbf{T}]$ are the influence matrices with a dimension of $(N+1)(2m+1)$ by $(N+1)(2m+1)$, $\{\mathbf{u}\}$ and $\{\mathbf{t}\}$ denote the column vectors of Fourier coefficients with a dimension of $(N+1)(2m+1)$ by 1 in which m indicates the truncated terms of Fourier series. For the circular-inclusion problem, multi-domain approach by taking the free body of each interface between the matrix and inclusions should be introduced. Therefore, an exterior problem for the matrix and several interior problems for each inclusion are needed to be solved by employing the null-field approach. The continuity of displacement and equilibrium of traction should be considered on the interface between the matrix and inclusions [8,9]. Then, the resulted linear algebraic system is obtained. After the boundary unknowns are solved, the field potential can be easily obtained according to Eq. (3).

Illustrative examples

1. Case 1: Infinite medium with two circular holes under the anti-plane shear (Laplace equation) A hole centered at the origin of radius a_1 and the other hole of radius $a_2 = 2a_1$ centered on x axis at $a_1 + a_2 + d$ are considered where d denotes the nearest distance between the holes. In order to be compared with the Honein *et al.*'s results [11] obtained by using the Möbius transformation, the stress along the boundary of radius a_1 is shown in Fig. 3 and good agreement is made.

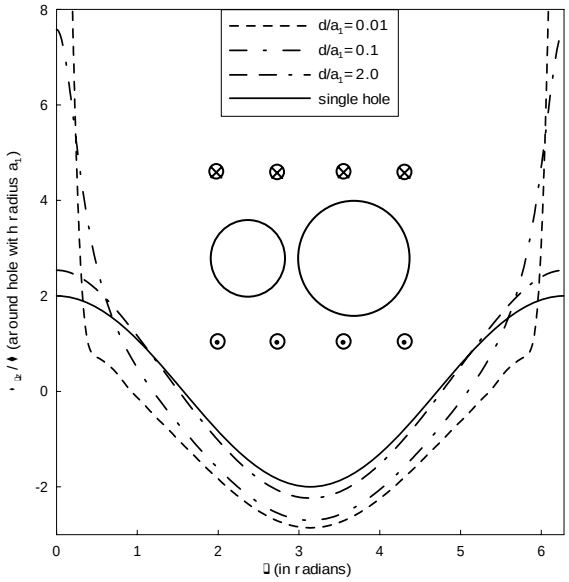

Figure 3: Stresses around the hole of radius a_1 **(Laplace equation)**

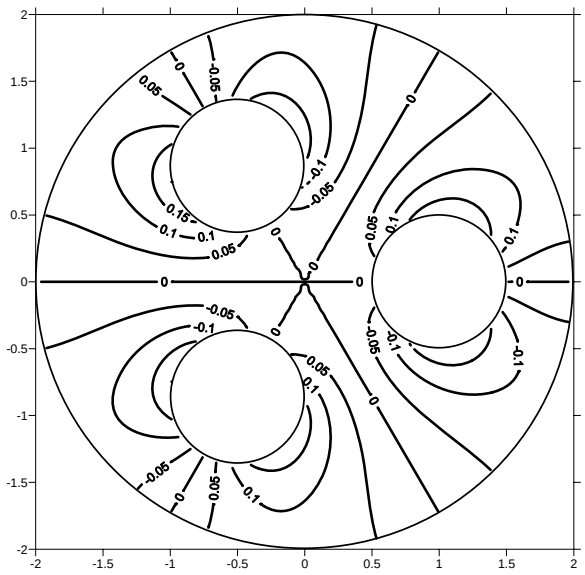

Figure 4: Displacement for the weakened circular bar by three holes **(Laplace equation)**

2. Case 2: A circular bar with three circular holes under torsion (Laplace equation) A circular bar with three equal circular holes removed is under torque at the end [12, 13]. The contour plot of the axial displacement is shown in Fig. 4. Good agreement is made after comparing with the Caulk's data [13]. Table 1 shows the comparison of the torsional rigidities G of three cases with different geometries of circular holes. The present solutions show improvement over Ling's results [12] in every case. The discrepancy in the second example in Table 1 may ascribe to the Ling's lengthy calculation in error as pointed out by Caulk [13].

Table 1 Torsional rigidity in Ling's examples

	Case	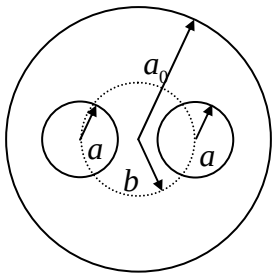	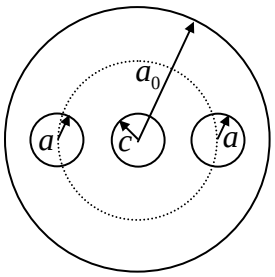	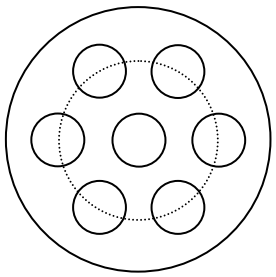
		$a/a_0=2/7, b/a_0=3/7$	$c/a_0=1/5, a/a_0=1/5,$ $b/a_0=3/5$	$c/a_0=1/5, a/a_0=1/5,$ $b/a_0=3/5$
$\frac{2G}{(\mu\pi a_0^4)}$	Caulk (First-order approximate)	0.8739	0.8741	0.7261
	Caulk (BIE formulation)	0.8713	0.8732	0.7261
	Ling's results	0.8809	0.8093	0.7305
	Present method ($m=10$)	0.8712	0.8732	0.7244

3. Case 3: A circular beam with two circular holes under bending (Laplace equation) Naghdi [14] and Bird and Steele [15] both calculated the stress concentration for the four equal-sized circular holes problem under bending. Bird and Steele [15] stated that the deviation by Naghdi's data is 11%. The grounds for this discrepancy were not identified in their paper. Our numerical results are more agreeable to the Naghdi's data as shown in Fig. 5. For the two equal-sized problems under bending, the stress concentration for

$d/a_1 = 0.125$ is shown in Fig. 6. Our numerical results are well compared with the Bird and Steele's data [15].

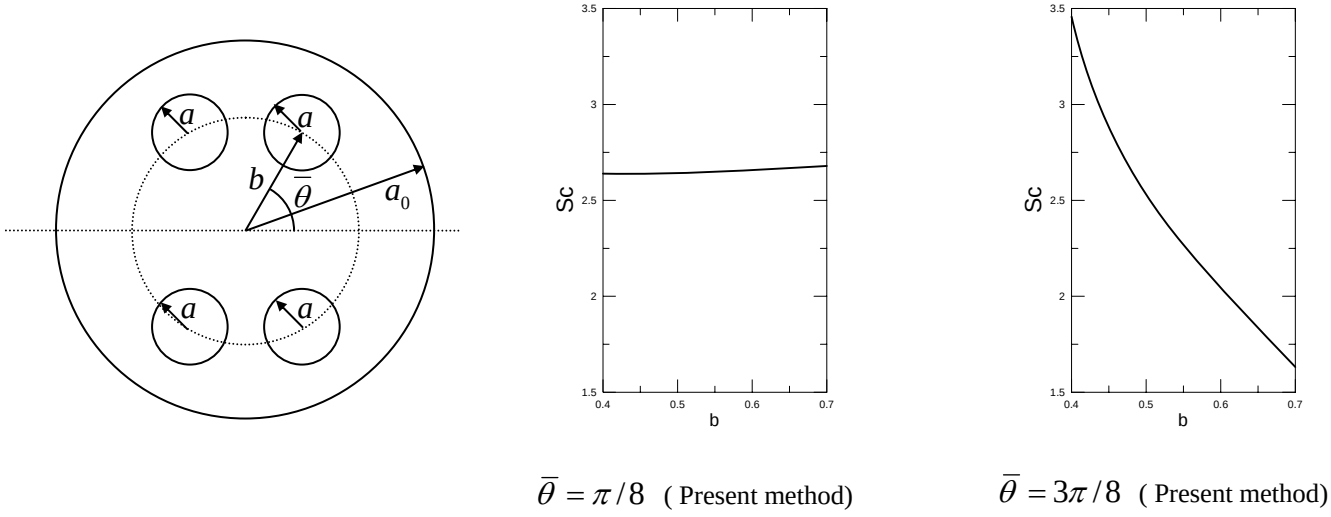

$\bar{\theta} = \pi/8$ (Present method) $\bar{\theta} = 3\pi/8$ (Present method)

Figure 5: Stress concentration versus b for $a = 0.12$ and $a_0 = 1.0$.**(Laplace equation)**

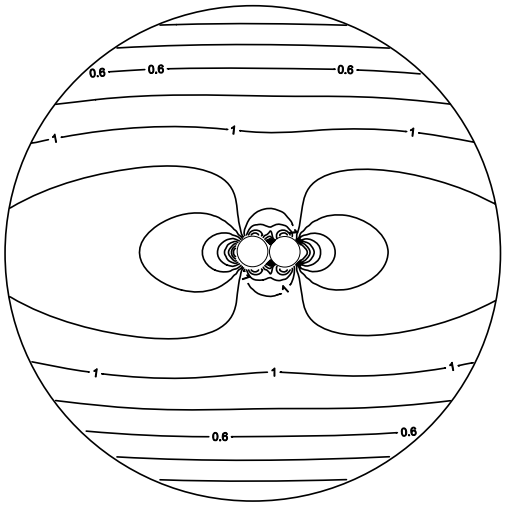

Figure 6: Contour of stress concentration for $d/a_1 = 0.125$ **(Laplace equation)**

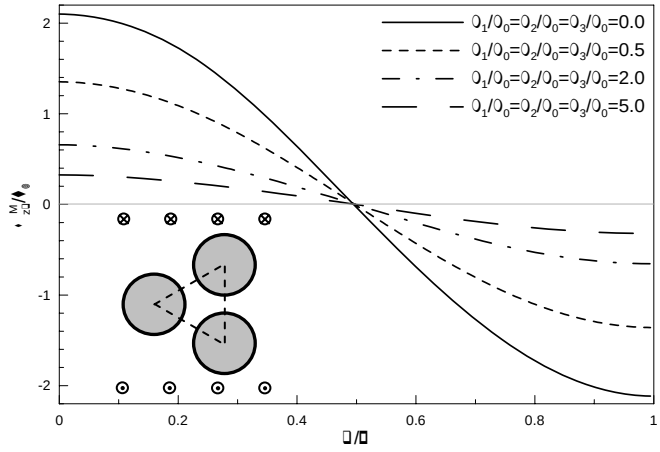

Figure 7: Tangential stress distributions around the inclusion located at the origin **(Laplace equation)**

4. Case 4: Infinite medium with three circular inclusions under the anti-plane shear (Laplace equation) Figure 7 shows that three identical inclusions subjected to the uniform shear stress $\sigma_{zy}^{\infty} = \tau_{\infty}$ at infinity. The three inclusions form an equilateral triangle and are placed at a distance $d = 2a_1$ apart. We evaluate the hoop stress $\sigma_{z\theta}$ in the matrix around the boundary of the inclusion located at the origin as shown in Fig. 7. Good agreement is obtained between the Gong's results [16] and ours. It is obvious that the limiting case of circular hole $(\mu_1/\mu_0 = \mu_2/\mu_0 = \mu_3/\mu_0 = 0.0)$ leads to the maximum stress concentration at $\theta = 0^{\circ}$, which is larger than 2 of a single hole due to the interaction effect.

5. Case 5: Piezoelectric problem with two circular inclusions under the anti-plane shear and in-plane electric field (Laplace equation) As the two circular inclusions are arrayed perpendicular to the coupled loadings of electrics and mechanics, the contour of shear stress σ_{zy} are plotted in Fig.8. The contour of shear stress matches very well with the Wang and Shen's results [17].

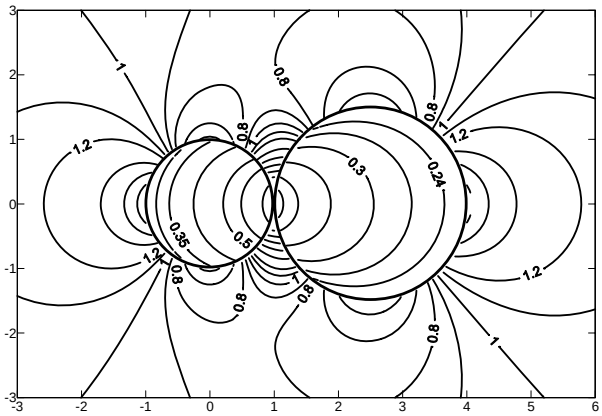

Figure 8: Contour of shear stress $\sigma_{zy}/\tau_{\infty}$
(Laplace equation)

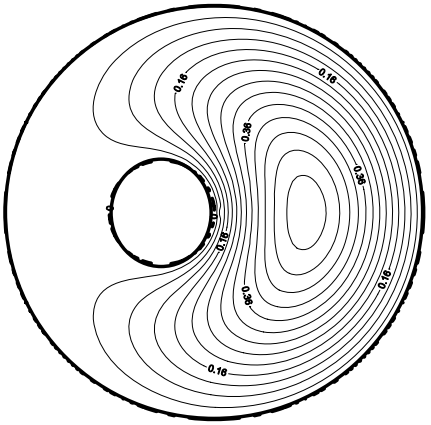

Figure 9: The first mode of eccentric membrane
(Helmholtz equation)

6. Case 6: Eigensolution for an eccentric membrane (Helmholtz equation) An eccentric case with radii a_1 and a_2 ($a_1 = 0.5, a_2 = 2.0$) is considered as shown in Fig. 9. The boundary condition is subject to the Dirichlet type. The result matches well with those of FEM and BEM.

7. Case 7: Eigensolution for an eccentric plate (bi-Helmholtz equation) An eccentric plate with radii a_1 and a_2 ($a_1 = 0.25, a_2 = 1.0$) is considered as shown in Fig. 10. The plate is fixed on the outer boundary and free inside. The result matches well with those of FEM and BEM [19].

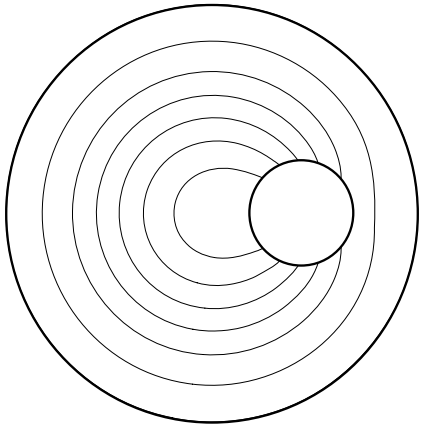

Figure 10: The first mode of eccentric plate
(biHelmholtz equation)

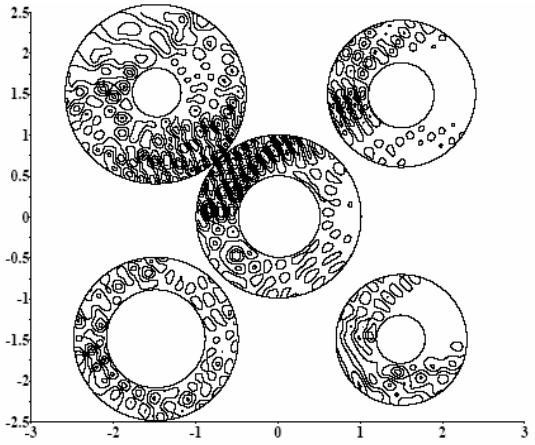

Figure 11: Contour of the real-part solution.
(Helmholtz equation-exterior acoustics)

8. Case 8: Five scatters of cylinders (Helmholtz equation-exterior acoustics) Plane wave scattering by five soft circular cylinders is solved by using the present method. The real-part solution in Fig.11 agrees well with that of multiple DtN method [20].

9. Case 9: A semi-cylindrical alluvial valley for the incident SH-wave (Helmholtz equation - half plane problem) A semi-cylindrical alluvial valley for the incident SH-wave is considered. Figure 12 shows the surface displacement for vertical incidence ($\gamma = 0^{\circ}$) of SH-wave versus the dimensionless frequency η. Agreement with the Trifunac's result [21] is obtained.

10. Case 10: Two semi-cylindrical alluvial valleys subject to the incident SH-wave (Helmholtz equation-half plane problem) Tsaur *et al*. [22] and Fang [23] both calculated the response of two semi-cylindrical alluvial valleys subject to the incident SH-wave. Tsaur *et al*. [22] pointed out that the error of Fang is due to abusing orthogonal properties. The amplitude versus x/a is shown in Fig.13 for the

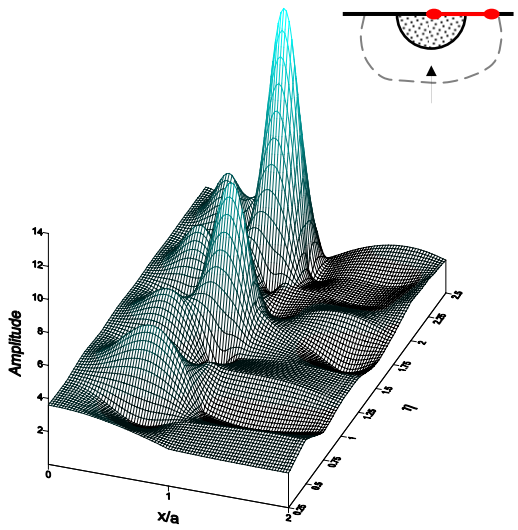

Figure 12: Surface displacements for the vertical incidence versus the frequency η **(Helmhotlz equation-half plane problems)**

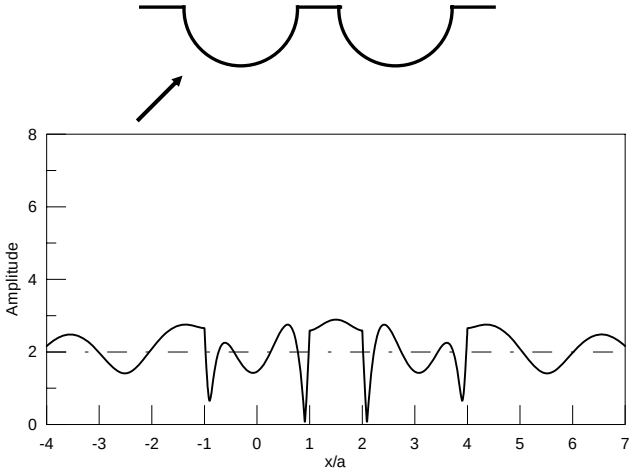

Figure 13: Amplitude versus two canyons subject to vertical incidence ($\gamma = 0^{\circ}$) with $\eta = 1$ **(Helmhotlz equation-half plane problems)**

vertical incidence ($\gamma = 0^{\circ}$). Good agreement is made after comparing our results with those of Tsaur *et al*. [22].

11. Case 11: An inclusion under the ground surface subject to the SH-wave (Helmholtz equation-half plane problem) Consider the half-plane problem with a circular inclusion under the ground surface subject to the SH-wave. Figure 14 shows the surface displacements of an inclusion problem under the ground surface subject to vertical incident SH-wave with $\eta = 2$. The surface displacements of the present method match well with the Tsaur's data [24], but it deviates to Manoogian and Lee's [25] result. The discrepancy was explained by Manoogian and Lee's [25] due to the precision limit in the FORTRAN code in 1996.

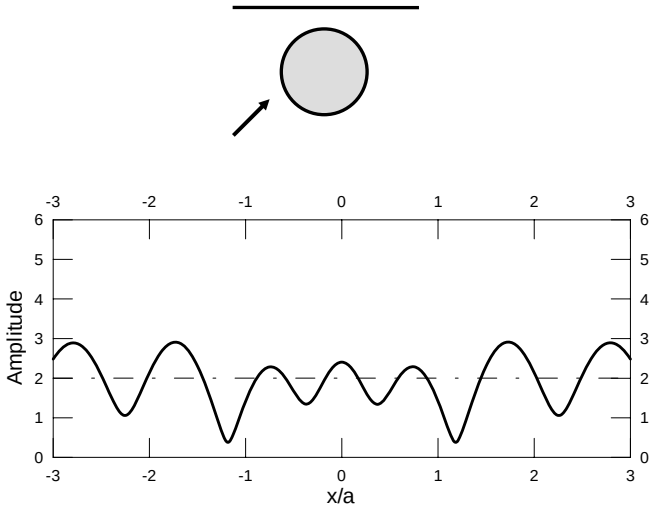

Figure 14: Surface displacements of an inclusion problem under the ground surface with $\eta = 2$ and $h/a = 1.5\,(\mu^I/\mu^M = 1/6, \rho^I/\rho^M = 2/3)$ **(Helmhotlz equation-half plane problems)**

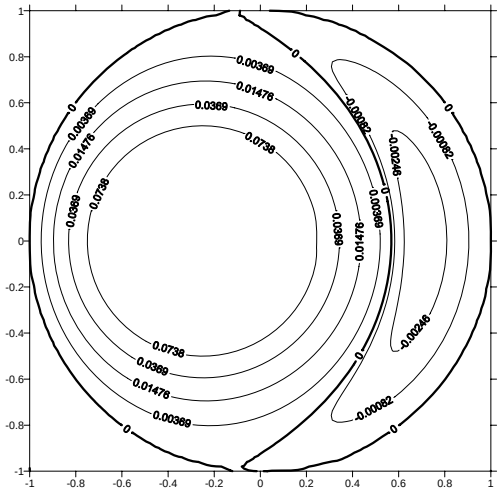

Figure 15: Stream function of Stokes' problem **(biharmonic equation)**

12. Case 12: Stokes' problem (biharmonic equation) An eccentric case of Stokes' flow problem is considered. The inner cylinder is rotating with a constant angular velocity and the outer one is stationary. The stream function is shown in Fig. 15 and matches well with that of BEM [26, 27].

Conclusions

A semi-analytical approach was proposed for solving BVPs with circular boundaries. Some recent results were reviewed. Although the BIE for the boundary point was employed, we need not to face the problems of *C.P.V*. and *H.P.V*. after introducing the degenerate kernel. Not only the singularity is transformed to the series sum but also the boundary-layer effect is eliminated. In order to verify the formulation, applications to the Laplace, Helmholtz, biharmonic and bi-Helmholtz problems were done. Five gains of well-posed model, singularity free, boundary-layer effect free, exponential convergence and mesh-free approach were achieved. Extension to other shapes, *e.g.* ellipse, as well as three dimensional problems is straightforward once the corresponding degenerate kernel is available.

Acknowledgements

The financial support from NSC project with Grants no. NSC 94-2211-E-019-009 as well as the numerical results implemented by the author's students, Mr. Wen-Cheng Shen, Mr. Chai-Tsung Chen, Mr. Chia-Chun Hsiao, Mr. An-Chien Wu, Mr. Po-Yuan Chen, Mr. Ying-Te Lee and the cooperator Dr. Wei-Ming Lee and Dr. Shyue-Yu Leu are highly appreciated.

REFERENCES

1. Lebedev NN, Skalskaya IP, Uflyand YS. *Worked Problem in Applied Mathematics*. Dover Publications, New York, USA, 1979.
2. Waterman PC. Matrix formulation of electromagnetic scattering. Proc. IEEE, 1965, vol. 53, pp. 805-812.
3. Doicu A, Wriedt T. Extended boundary condition method with multiple sources located in the complex plane. Optics Commun., 1997; **139**: 85-91.
4. Chen JT, Shen WC, Wu AC. Null-field integral equations for stress field around circular holes under anti-plane shear. Engineering Analysis with Boundary Elements, 2005; **30**: 205-217.
5. Chen CT. *Null-Field Integral Equation Approach for Helmholtz (Interior and Exterior Acoustic) Problem with Circular Boundaries*. Master Thesis, Department of Harbor and River Engineering, National Taiwan Ocean University, Taiwan, 2005.
6. Chen JT, Hsiao CC, Leu SY. Null-field integral equation approach for plate problems with circular holes. ASME J. Appl. Mech., 2006; **73**: 679-693.
7. Chen JT, Shen WC, Chen PY. Analysis of circular torsion bar with circular holes using null-field approach. Computer Modelling in Engineering Science, 2006; **12**: 109-119.
8. Chen JT, Wu AC. Null-field approach for multi-inclusion problem under anti-plane shears. ASME J. Appl. Mech., 2006 (accepted).
9. Chen JT, Wu AC. Null-field approach for piezoelectricity problems with arbitrary circular inclusions. Engineering Analysis with Boundary Elements, 2006, (accepted).
10. Chen JT. Null filed integral equation approach for boundary vale problems with circular boundaries. Keynote lecture of ICCES 2005, India, 2005.
11. Honein E, Honein T, Herrmann G. On two circular inclusions in harmonic problems. Quarterly of Applied Mathematics, 1992; **50**: 479-499.
12. Ling CB. Torsion of a circular tube with longitudinal circular holes. Quarterly of Applied Mathematics, 1947; **5**: 168-181.
13. Caulk DA. Analysis of elastic torsion in a bar with circular holes by a special boundary integral method. ASME Journal of Applied Mechanics, 1983; **50**: 101-108.
14. Naghdi AK. Bending of a perforated circular cylindrical cantilever. International Journal of Solids and Structures. 1991; **28**: 739-749.

15. Bird MD, Steele CR. A solution procedure for Laplace's equation on multiply connected circular domains. ASME Journal of Applied Mechanics. 1992; **59**: 398-404.
16. Gong SX. Antiplane interaction among multiple circular inclusions. Mechanics Research Communications, 1995; **22**: 257-262.
17. Wang X, Shen YP. On double circular inclusion problem in antiplane piezoelectricity. International Journal of Solids and Structures, 2001; **38**: 4439-4461.
18. Chen JT, Lin JH, Kuo SR, Chyuan SW. Boundary element analysis for the Helmholtz eigenvalue problems with a multiply connected domain. Proc. R. Soc. Lond. A, 2001; **457**: 2521-2546.
19. Lee WM, Chen JT, Lee YT. Free vibration analysis of circular plates with multiple circular holes using indirect BEMs. The Fourteenth Annual Conference on Vibration and Acoustics, Ilan, Taiwan, 2006.
20. Grote MJ, Kirsch C. Dirichlet to Neumann boundary conditions for multiple scattering problems. J. Comp. Physics, 2004; **201**: 630-650.
21. Trifunac MD. Surface motion of a semi-cylindrical alluvial valley for incident plane SH waves. Bulletin the Seismological Society of America, 1971; **61**: 1755-1770.
22. Tsaur DH, Chang KH, Lin JG. Response of multiple semi-circular cylindrical canyons subject to plane SH-waves. Asia Pacific Review of Engineering Science and Technology, 2004; **2**(2): 251-266.
23. Fang YG. Scattering of plane SH-waves by multiple circular-arc valleys at the two-dimensional surface of the earth. Earthquake Engineering and Engineering Vibration, 1995; **15**(1): 85-91.
24. Tsaur DH, Chang KH. 2006, (private communication).
25. Manoogian ME, Lee VW. Diffraction of SH-waves by subsurface inclusions of arbitrary shape. Journal of Engineering Mechanics, 1996; **122**(2): 123-129.
26. Kelmanson MA. *Boundary Integral Equation Analysis of Singular, Potential and Biharmonic Problems*. PhD Thesis, Department of Applied Mathematics, University of Leeds, 1983.
27. Ingham DB, Kelmanson MA. *Boundary Integral Equation Analyses of Singular, Potential, and Biharmonic Problems*. Lecture notes in engineering, vol. 7, Springer-Verlag, Berlin, Heidelberg, Germany, 1984.